

Supplementary Materials

Ultrasensitive Mid-Infrared Detection through Ligand-Driven Local Heating in Lanthanide- doped Nanoparticles

Chong Wu Wang^{1†}, Liangliang Liang^{3†}, Xuran Zhang¹, Mingjin Dai¹, Jiaye Chen²,
Xiaogang Liu^{2*}, Qi Jie Wang^{1,4*}

Materials: Sodium hydroxide (NaOH; >98 %), ammonium fluoride (NH₄F; >98 %), 1-octadecene (90 %), oleic acid (90 %), yttrium acetate hydrate (Y(CH₃CO₂)₃·x H₂O; 99.9 %), neodymium acetate hydrate (Nd(CH₃CO₂)₃·x H₂O; 99.9 %), ytterbium acetate hydrate (Yb(CH₃CO₂)₃·x H₂O; 99.9 %), cyclohexane (>98 %), and methanol (>99 %) were all purchased from Sigma–Aldrich and used as received without further purification.

Synthesis. Specially designed Nd³⁺-Yb³⁺ doped nanocrystals were synthesized by a modified co-precipitation method. In a typical procedure, an aqueous solution (4.0 mL) of Nd(CH₃CO₂)₃, Yb(CH₃CO₂)₃ and Y(CH₃CO₂)₃ in various molar ratios was added to a 50-mL flask containing 6.0 mL of oleic acid and 14.0 mL of 1-octadecene. The mixture was heated to 150 °C and kept for 60 min to form lanthanide-oleate coordination complexes. After cooling down to 50 °C, a methanol solution (12.0 mL) containing NH₄F (3.2 mmol) and NaOH (2.0 mmol) was added under stirring at 50 °C for 60 min. The solution was then heated to 100 °C and kept under vacuum for 20 min to remove the volatile residue. The remaining mixture was heated to 290 °C and maintained at this temperature for three hours under an inert nitrogen environment. After cooling to room temperature, the resulting nanocrystals were collected by centrifugation, washed several times with ethanol, and dispersed in 4.0 mL of cyclohexane for further treatment.

Lanthanide nanotransducer films were prepared using a simple drop-casting method. Specifically, 20 µL of ethanol solution (10 mg/mL) was dropped onto a BaF₂ substrate placed in a Petri dish. This process is repeated to increase the thickness of the film.

Characterization. The sizes and morphologies of the as-prepared nanocrystals were characterized using a transmission electron microscope (JEOL-1400 TEM) operating at an acceleration voltage of 100 kV. Powder X-ray diffraction (XRD) patterns were recorded by an X-ray diffractometer (ADDS) with Cu/Kα radiation (40 kV, 40 mA, λ=1.54184 Å).

Customized fluorescence system was utilized to examine the MIR radiation response of the lanthanide nanotransducers. A multimode laser operating at 740 nm (CNI-MDL-III) was used as the excitation process. This light was directed by a dichroic long-pass filter with a cut-off at 760 nm (Newport HPD760, Newport) and concentrated onto the nanotransducer film via a 50X objective lens (Mitutoyo, NA 0.55). The tunable quantum cascade laser (QCL) from 4.4 to 10 micrometers (Daylight Solutions, MIRcat), was applied as the MIR source, with the beam precisely focused onto the film by a zinc selenide (ZnSe) lens with a 5 cm focal length (Thorlabs)

The lifetime of the lanthanide particle was measured in the same system, a Si APD was used to collect NIR emission (APD430A, 400MHz). The band pass filter around 805, 860 and 980 nm was used to filter the emission band. An oscilloscope (Tektronix, TBS1000C) was connected to the APD to get the electrical signal. The function generator provide the analogy signal

For luminescence of the film was recorded by a CCD spectrometer (Witec) with a 750-nm long-pass filter. The integration time was set as 10 ms. The emission power can be detected and measured with a Si amplified detector (Thorlabs, PDA36A2). The 950 nm long pass filter was placed in front of the detector to filter the emission for Yb^{3+} . The output voltage was connected to a high-sensitivity digital source meter (Keysight, 2912A). The MIR laser power was measured using a thermal power meter (OPHIR, Nova display-ROHS). The noise spectra are recorded with a Keysight PXA Signal Analyzer (N9030B).

For the calculation of MIR transducing efficiency, the power of the reduced emission around 980 nm was recorded with an amplified Si detector (Thorlabs, PDA36A2). Considering the transmission of the objective (65%), dichroic filter (89%) and lens (91%), an overall collection efficiency of less than 4% can be estimated. The following expression was used to calculate external and internal quantum efficiencies for MIR-to-NIR transduction.

$$\eta_{External} = \frac{Power_{NIR}/(h\nu_{NIR})}{Power_{MIR\ input}/(h\nu_{MIR})}$$

The gas spectroscopy measurement is performed using a 20 cm length gas cell. The MIR light is modulated by an optical chopper with frequency set as 100-200 Hz. For comparison, the transmitted light is tested with a commercial pyroelectric sensor (Shimadzu, MTG-22). Alternatively, the light is focused on the lanthanide film. The emission goes through the band pass filter (980 nm or 805 nm), and is measured with the Si detector (Thorlabs, PDA36A2). The output signal is demodulated by the lock-in amplifier (Zurich Instrument, HF2LI).

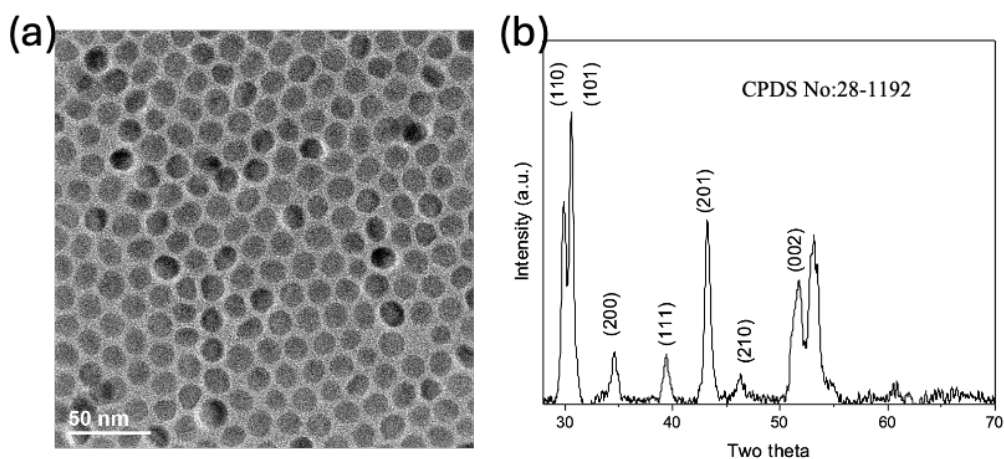


Fig. S1 | Morphology and crystal structure of Nd/Yb co-doped NaYF₄ nanocrystals. (A) The transmission electron microscopy (TEM) image show the size of the particles is around 20 nm. and (B) X-Ray diffraction (XRD) pattern for the lanthanide nanoparticles, which is match well with JCPDS No:28-1192 for β -NaYF₄

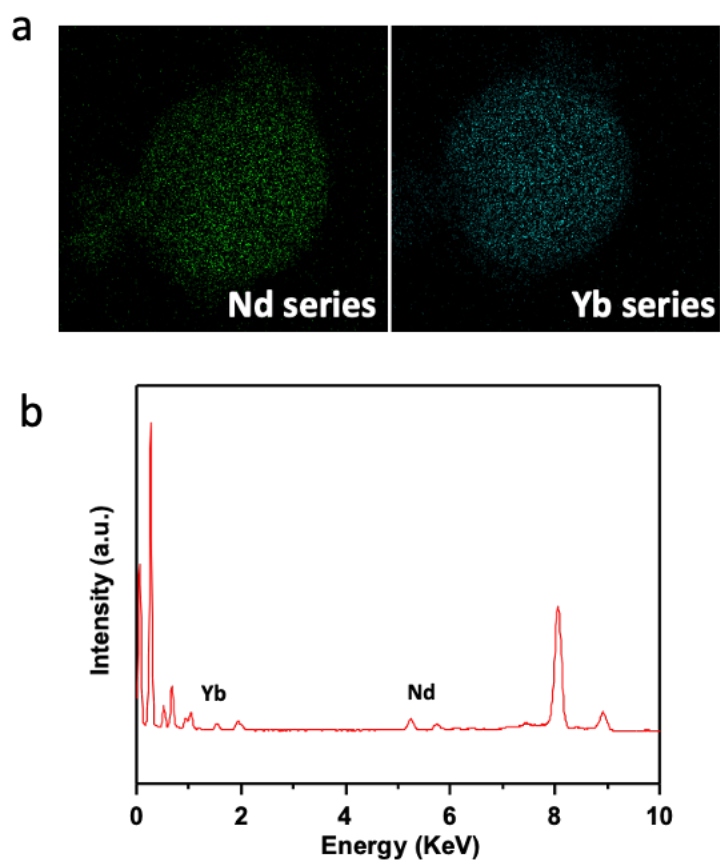


Fig. S2 | Element analysis for prepared nanocrystals. (a) The TEM-EDS mapping for Nd and Yb. The lanthanide ions are uniformly distributed in the crystal. (b) EDS spectra for lanthanide particles confirm the doping of Nd^{3+} and Yb^{3+} .

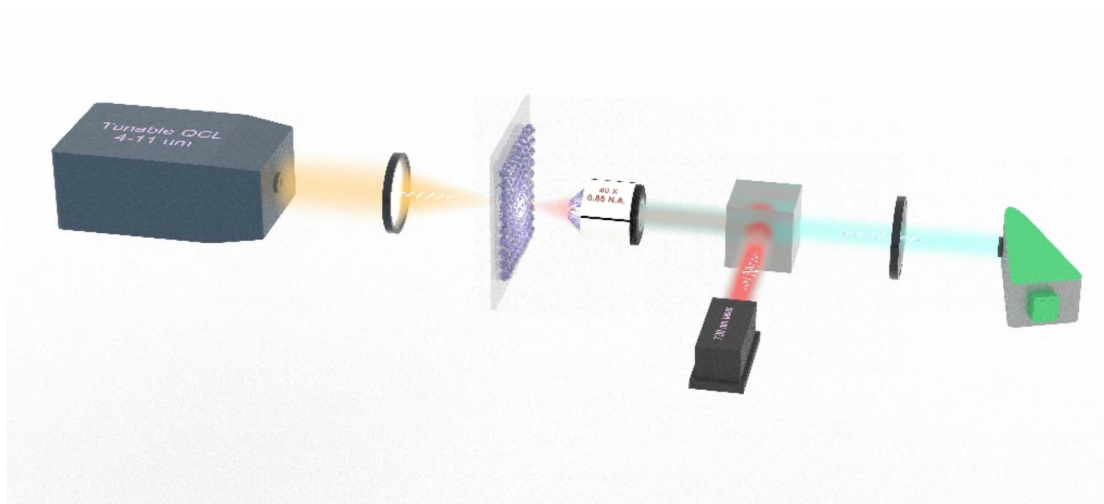


Fig. S3 | The experiment setup for MIR upconversion measurement. The tunable QCL (5-10 μm) is used as the MIR source. The 730 nm laser is used as NIR source. Two beams focus and collimate from two sides of the nanofilm. The luminance is collected by a CCD spectrometer.

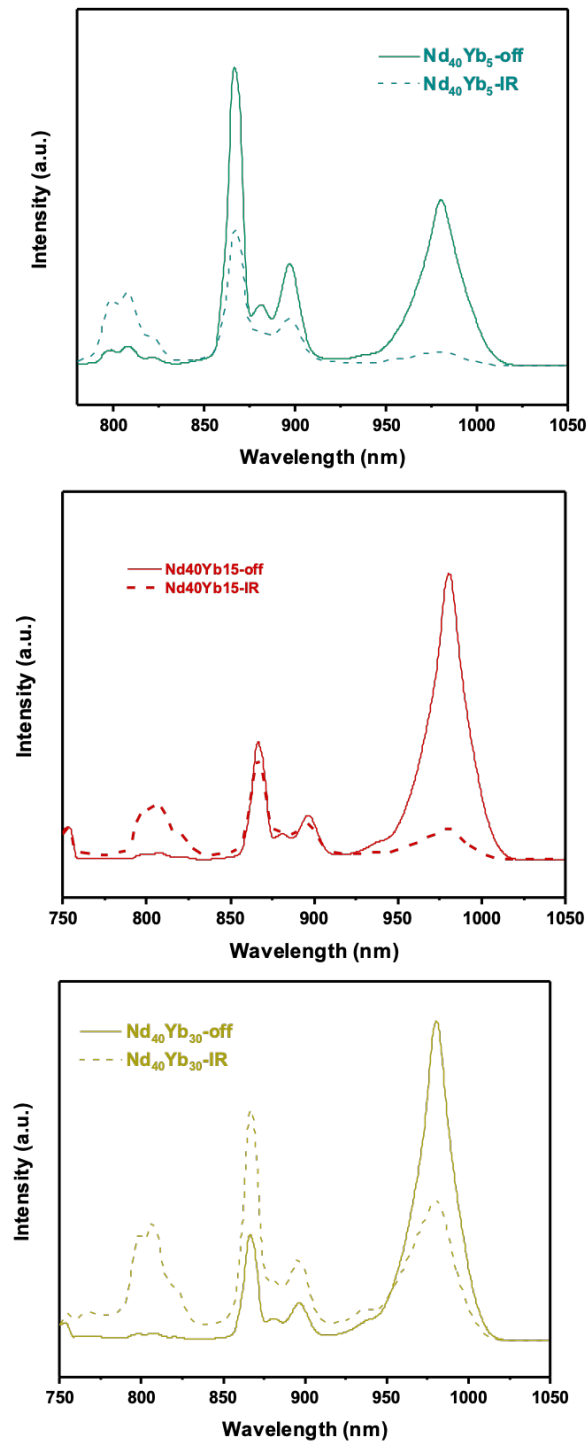


Fig. S4 The PL spectra response for nanocrystals with different compositions. Both spectra are recorded with and without MIR radiation (6.3 μm , 25 mW) for NaYF₄:Nd₄₀Yb₅, NaYF₄:Nd₄₀Yb₁₅, and NaYF₄:Nd₄₀Yb₃₀.

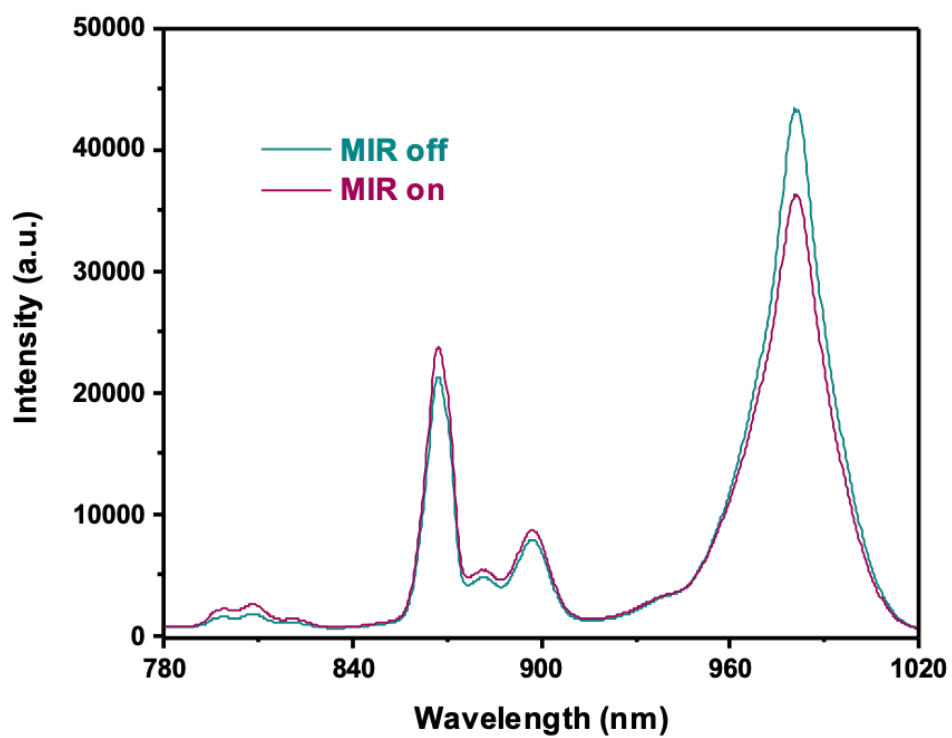


Fig. S5 | The MIR sensitivity for ligand free samples. The photoluminescence spectra for ligand free-NaYF₄:Nd₄₀Yb₁₅ nanocrystals with and without MIR radiation (6.3 μ m, 35 mW).

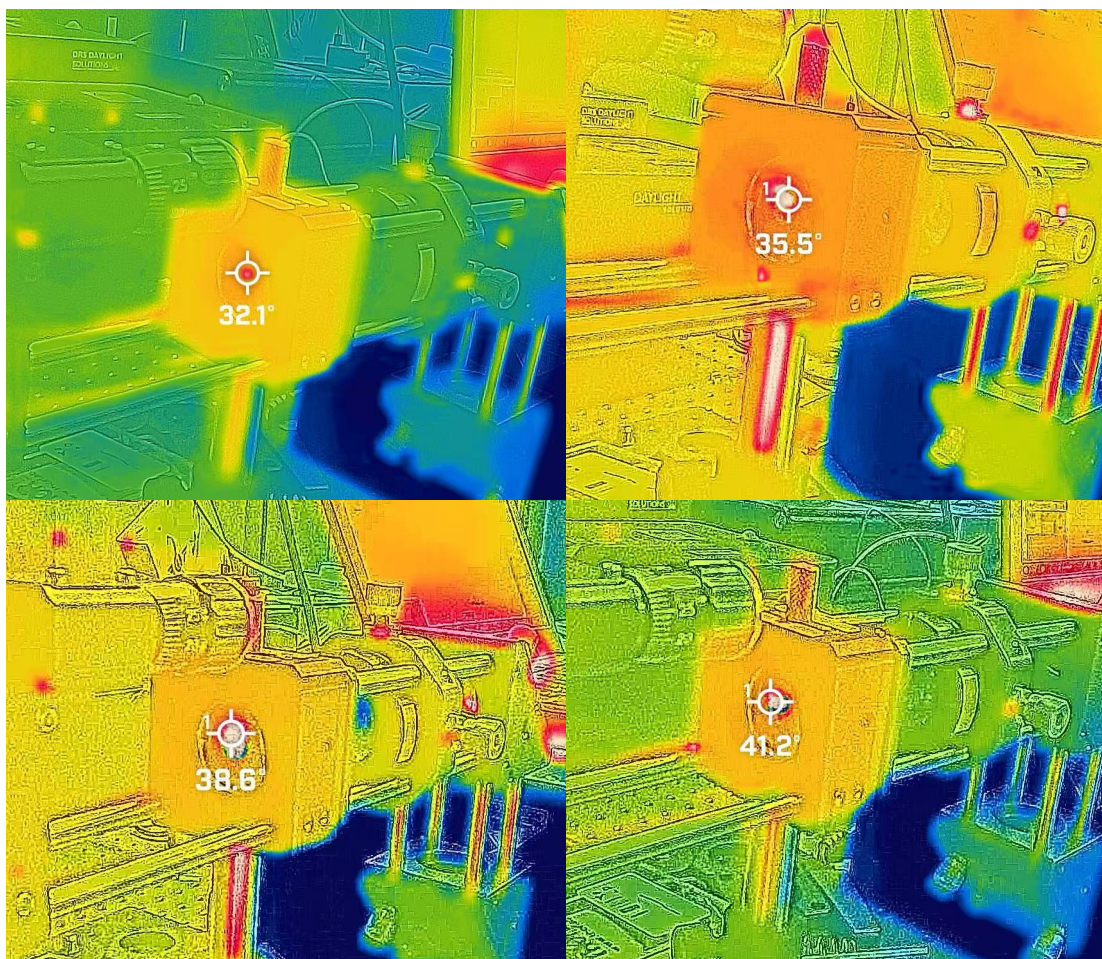


Fig. S6 | Temperature recorded for lanthanide film under different MIR power radiation. (0.3-2.4 mW)

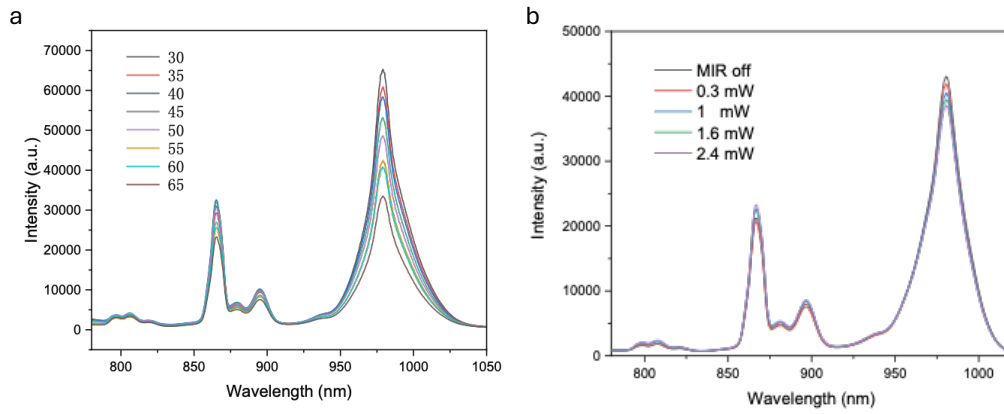


Fig. S7 | Temperature-dependent fluorescence response of NaYF₄:Nd₄₀Yb₁₅. (a) The PL emission spectra at different temperatures 30-65 degrees. (b) The PL emission spectra under different MIR powers.

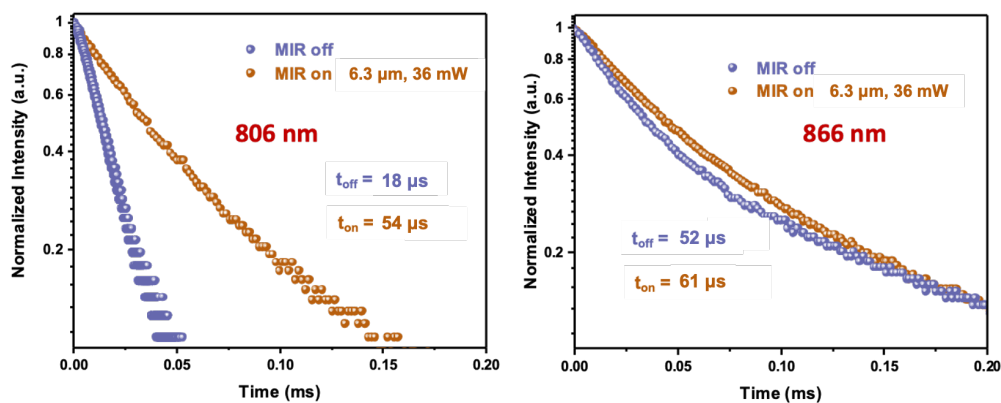


Fig. S8 | Lifetime measurement for different Nd^{3+} energy levels. The transient PL measurement for 806 and 866 nm emissions with and without MIR radiation. The increased lifetime for $^4\text{F}_{5/2}$ of Nd^{3+} is consistent with the enhanced 806 nm emission.

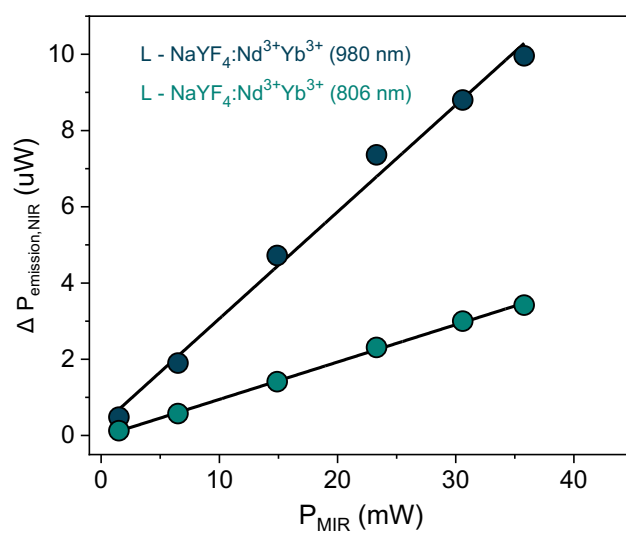


Fig. S9 | The change of NIR emission power (980 nm and 806 nm) for NaYF₄:Nd₄₀Yb₁₅ under different MIR powers.

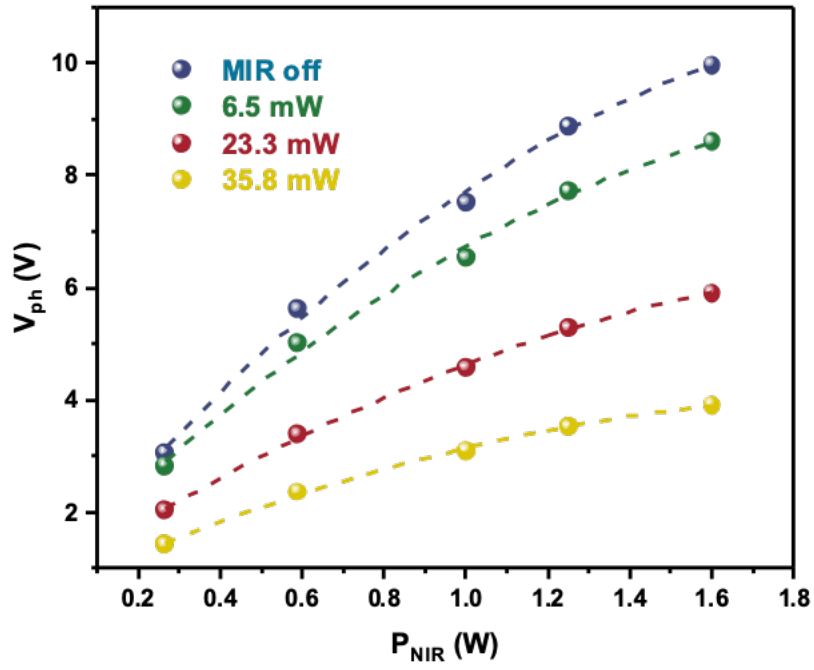


Fig. S10 | Characterization of NIR pumping power on MIR upconversion detection. The voltage of Si detector increases with the NIR laser power and starts to saturate at around 1.6 W.

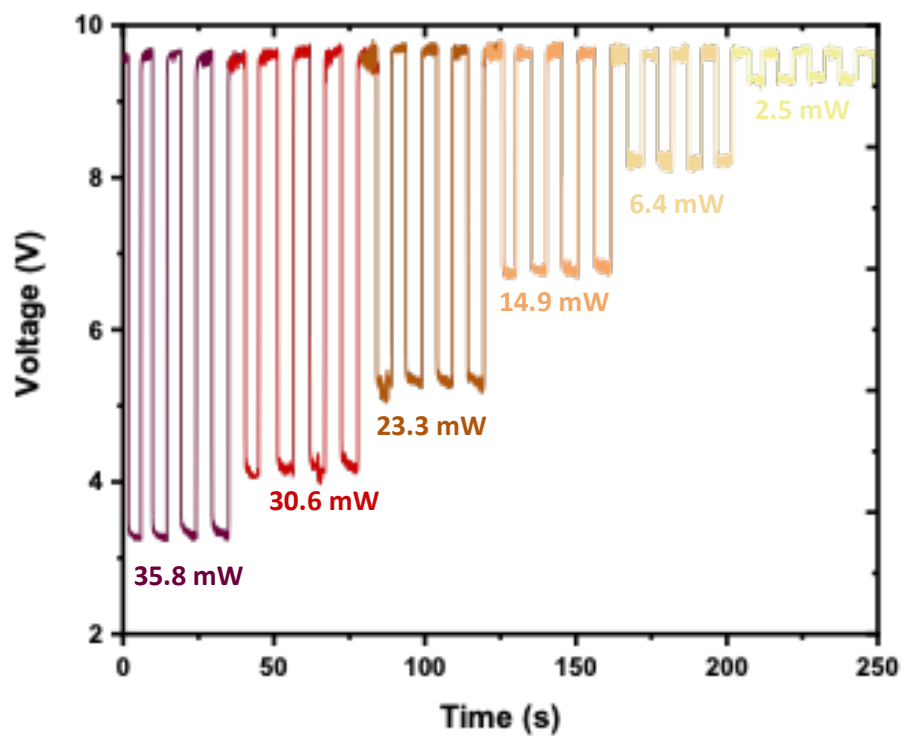


Fig. S11 | Characterization of power dependent MIR upconversion detection. The time-resolved photovoltage responses recorded under multiple periodic switches of laser illuminations from 35.8 to 2.5 mW.

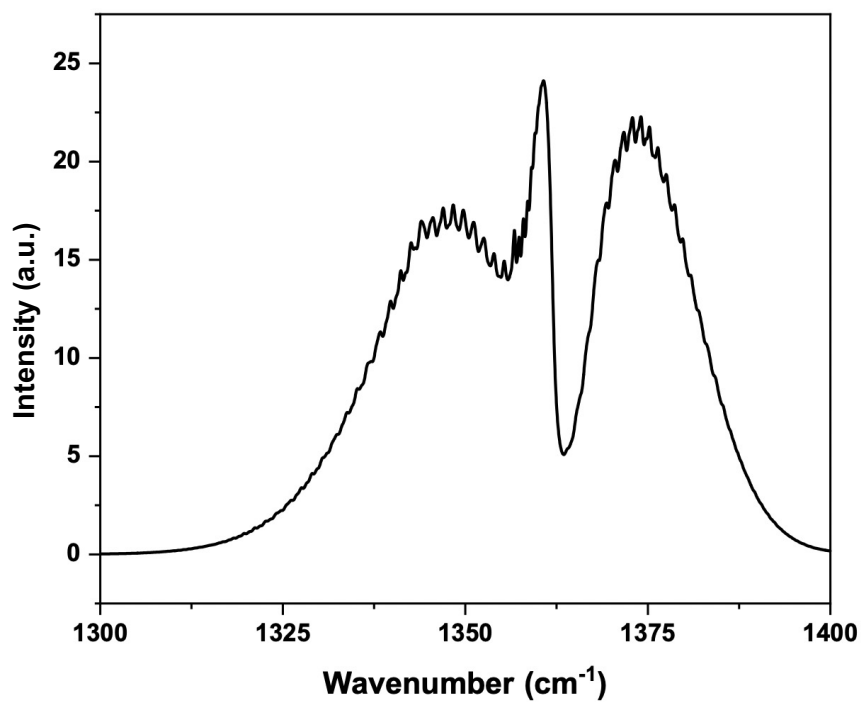


Fig. S12 | The absorption spectra for SO₂ from Hitran database. The calculated spectrum is consistent with the spectra obtained with the MIR upconversion module.